Insights into the mechanism of activation of the phosphorylation-independent response regulator NblR. Role of residues Cys69 and Cys96

Javier Espinosa [1,a], Maria-Luisa Lopez-Redondo [1,b], José L. Neira [c,d], Alberto Marina[b,*] and Asunción Contreras[a,*]

[a]División de Genética, Universidad de Alicante, Apartado 99, E-03080 Alicante, Spain

[b] Instituto de Biomedicina de Valencia (CSIC) and CIBERER, 46010 Valencia, Spain

[c] Instituto de Biología Molecular y Celular, Universidad Miguel Hernández, 03202 Elche (Alicante), Spain

[d] Instituto de Biocomputación y Física de los Sistemas Complejos (BIFI), 50009 Zaragoza, Spain

*Corresponding authors addresses. Asunción Contreras, División de Genética, Universidad de Alicante. Apdo 99; 03080 Alicante (Spain). Phone: + 34 96 5903957 Fax: + 34 96 5909469). Email: contrera@ua.es

Alberto Marina, Unidad de Cristalografía de Macromoléculas, Instituto de Biomedicina de Valencia (CSIC), Jaime Roig 11, 46010 Valencia (Spain). Phone: +34-963391754. Fax: +34-963690800. Email: amarina@ibv.csic.es.

[1]The first two authors contributed equally to this work.

Abstract

Cyanobacteria respond to environmental stress conditions by adjusting their photosynthesis machinery. In *Synechococcus* sp. PCC 7942, phycobilisome degradation and other acclimation responses after nutrient or high light stress require activation by the phosphorylation-independent response regulator NblR. Structural modelling of its receiver domain suggested a role for Cys69 and Cys96 on activation of NblR. Here we investigate this hypothesis by engineering Cys to Ala substitutions. *In vivo* and *in vitro* analyses indicated that mutations Cys69Ala and/or Cys96Ala have a minor impact on NblR function, structure, size, or oligomerization state of the protein, and that Cys69 and Cys96 do not seem to form disulphide bridges. Our results argue against the predicted involvement of Cys69 and Cys96 on NblR activation by redox sensing.

Keywords: stress response, NblR, cyanobacteria, cysteine, response regulator, structure.

Abbreviations used: CD, circular dichroism; *nblA*, non-bleaching protein A; *nblR*, non-bleaching protein R; $NblR^{C69A}$, the alanine mutant of NblR at position 69; $NblR^{C96A}$, the alanine mutant of NblR at position 96; RR, response regulator; PIARR, Phosphorylation-Independent Activation of Response Regulator.

1. Introduction

Cyanobacteria, photosynthetic prokaryotes that perform plant-type oxygenic photosynthesis, have developed mechanisms to modify the composition of the photosynthetic machinery in response to environmental changes [1]. One dramatic example of this adaptation is the process of chlorosis or bleaching, degradation of the light-harvesting antennae, the phycobilisomes, under stress conditions such as nutrient starvation [2]. High levels of *nblA* gene expression (non-bleaching protein A) are required for phycobilisome degradation [3]. The loss of phycobilisomes and a reduction of the chlorophyll content during stress conditions are responsible for the yellow appearance of chlorotic cultures. Degradation of phycobilisomes avoids excessive absorption of excitation energy and supplies the cell with amino acids for the synthesis of proteins required for acclimation and cell survival [4].

NblR have been implicated in general adaptation to stress in *Synechococcus* sp. PCC 7942 (hereafter *S. elongatus*) [5]. Orthologues of the response regulator (RR) NblR appear in very few cyanobacterial species [6]. NblR is required for the strong increase on *nblA* gene expression observed during nutrient stress in *S. elongatus* [5, 7-9]. Although there are indications of a role for NblR in down-regulation of photosynthetic electron transport under stress conditions [5], the mechanism and components involved in NblR activation remain to be elucidated. In this context, interactions of NblR with other proteins have been identified using yeast two-hybrid approaches, but their functional relevance remains to be investigated [10-12].

Sequence homology classifies NblR with the OmpR/PhoB subfamily of two-component RRs. Upon phosphorylation of typical response regulators (RRs) of this family, a conserved Thr/Ser residue (absent in NblR) is hydrogen-bonded with the phosphoryl group, inducing the repositioning of the loop that connects the β4 strand with the α4 helix and the concomitant orientation inwards of an exposed aromatic residue in β5 (Tyr104 in NblR). This orchestrated movement, referred to as the "T-loop-Y" switch, leads to receiver dimerization [13]. Contrary to *bona fide* two-component RRs,

NblR is not regulated by phosphorylation and it has been grouped with other atypical RRs into the PIARR (Phosphorylation-Independent Activation of Response Regulator) class [10]. These proteins maintain a high degree of amino acid conservation and most of the structural features of canonical RRs, but differ at particular key residues and are not regulated by phosphorylation.

NblR shares ten out of the eleven conserved residues of the α4-β5-α5 surface that are involved in the phosphorylation-induced dimerization characteristic of the OmpR/PhoB family [14, 15]. While *Helicobacter pylori* hp1043 and *Chlamydia trachomatis* ChxR, also PIARR members of this family, are constitutive homodimers [16, 17] NblR is monomeric [10], prompting the question of whether NblR activation also requires dimerization.

Because NblR is not regulated by phosphorylation [10], alternative signalling mechanisms must be required for activation of this atypical RR under a variety of stress conditions. From a structural model of the NblR receiver domain (Fig. 1), it was proposed that activation would involve redox sensing and a disulphide bridge between Cys96 of helix α4, a key structural element in the activation-induced dimerization surface, and Cys69 of helix α3 [10]. Here, we use a combination of *in vivo* and *in vitro* approaches to test this hypothesis, and to get insight into the function of the two cysteine residues.

2. Materials and Methods

2.1. Molecular genetic techniques and culture conditions

Cloning procedures were carried out with *Escherichia coli* DH5α, using standard techniques. *S. elongatus* strains were grown at 30 ºC under constant illumination (40 µmol photons m^{-2} s^{-1}) provided by cool white fluorescent lights. For liquid media $BG11_0$ (without added nitrogen source), BG11 ($BG11_0$ containing 17.5mM $NaNO_3$ and 10mM Hepes/NaOH pH 7.8) or $BG11_{-s}$ (BG11 in which $MgSO_4$ was substituted with an equimolar amount of $MgCl_2$), as described [18]. For growth on plates, the medium was solidified by addition of 1% (w/v) agar.

S. elongatus strains were transformed essentially as described [19]. The antibiotics kanamycin (10 µg ml^{-1}), chloramphenicol (5 µg ml^{-1}) or streptomycin (5 µg ml^{-1}) were added to the selection plates.

For initiation of stress experiments (nitrogen or sulfur starvation) cells were grown on BG11 until they reached mid-exponential phase. At this point, cells were harvested by centrifugation, washed twice with BG11 lacking either nitrate or sulfur, and resuspended in the same media.

2.2 Construction of mutant strains and plasmids

In all cases, the introduced mutations were confirmed by DNA sequencing. Oligonucleotides used are listed in Supplementary Table.

A *Hinc*II–*Eco*RV fragment containing the C.S3 cassette from pUAGC453 was cloned into the Klenow-treated *Sty*I site of pUAGC235 [10], giving plasmid pUAGC236. Downstream sequences of *nblR* (670 bp) were amplified from genomic *S. elongatus* DNA using primers NblR-down-4F and NblR-down-4R. The PCR product was then cut with *Hind*III and *Hinc*II and Klenow filled. This blunt fragment was then cloned into *Hinc*II-cut pUAGC236, giving plasmid pUAGC237, carrying the C.S3 cassette between *nblR* and the ORF Synpcc7942_2306.

Quick change mutagenesis reactions (Stratagene, USA), independently performed with primer pairs NblR-C69A-F/NblRC69A-R or NblR-C96A-F/NblRC96A-R, using plasmid pUAGC237 as template, resulted in plasmids pUAGC733 and pUAGC734, respectively. For double mutation, pUAGC733 was used as a template in a new Quick change mutagenesis reaction using NblR-C96A-F/NblRC96A-R as primers, resulting in plasmid pUAGC735. Similarly, plasmids pENS38_1 and pENS38_2, encoding NblR^{C69A} and NblR^{C96A} were derived from pENS38 [10].

After transformation of pUAGC733, pUAGC734 and pUAGC735 into *S. elongatus*, stable chromosomal integration of the C.S3 cassette in the expected location was confirmed by PCR with primers NblR-1F and CS3-2F. The presence of either *nblR* mutant or wild-type alleles was checked by sequencing of the PCR product obtained with primers NblR-1F and NblR-1R. A clone of each type was selected for further analysis (control strain: WT-RCS3, mutant strains: NblR^{C69A}-RCS3, NblR^{C96A}-RCS3 and NblR$^{C69A/C96A}$-RCS3).

To generate control and *nblR* mutant strains carrying the P$_{nblA}$::*luxAB* reporter fusion, plasmid pUAGC103 was transformed independently into NblR45, WT-RCS3, NblR^{C69A}-RCS3, NblR^{C96A}-RCS3 and NblR$^{C69A/C96A}$-RCS3 [20]. The presence of *nblA*::*luxAB* transcriptional fusion on selected clones was confirmed by PCR with primers pAM1580seq and nblA1F.

2.3 Determination of pigment contents spectrophotometrically

1 ml of cultures at OD_{750} 0.5 were taken at the indicated times, diluted with fresh medium to, and whole-cell absorbance spectra (500–800 nm) were recorded on a UV/VisibleUltrospec 2100 pro (GE Healthcare, Spain). Pigment content was determined as described [20].

2.4 Determination of luciferase activity

1 ml of cultures grown to mid-exponential phase were adjusted to an OD_{750} of 0.5 and supplemented with decanal to a final concentration of 0.25 mM from a 50 mM stock solution made up in 10% DMSO. Light emission was recorded in a Perkin Elmer Viktor3 luminometer. Bioluminescence measurements were carried out as described [20].

2.5 Protein expression and purification

Plasmids pENS38, pENS38_1, and pENS38_2 were transformed into the *E. Coli* strain BL21-codonPlus (DE3)-RIL (Stratagene) and the corresponding cultures were grown at 37 ºC in LB supplemented with amplicilin (100 μg ml^{-1}) and cloramphenicol (33 μg ml^{-1}) to an OD_{600} of 0.15-0.2. The incubation was then continued at 25 ºC till an OD_{600} ~0.5 was reached, and then, 1 mM IPTG (isoproplyl-1-thio-galactopyranoside) was added. After 4 hours of incubation at 25ºC cells were harvested by centrifugation, resuspended in A buffer (50 mM Tris-HCl pH 8.0, 150 mM NaCl, 5% Glycerol) supplemented with 1 mM phenylmethylsulphonyl fluoride (PMSF), and disrupted by sonication. Unbroken cells and cell debris were removed by centrifugation at 18.000 *g* for 30 min at 4 °C. The supernatants were loaded onto HisTrap FF column (GE Healthcare) equilibrated in A buffer, and the proteins were eluted with buffer A supplemented with 200 mM of imidazol. The purest fractions, as determined by SDS-PAGE and Coomassie Blue staining, were pooled and submitted to a size exclusion chromatography using a Sephadex 75 16/60 column (GE Healthcare) equilibrated with buffer A running on an AKTA FPLC system (GE Healthcare), detecting the absorbance at 280 nm. Again, the purest fractions were pooled, concentrated using Amicon (Millipore) and stored at -80ºC.

2.6. Analytical size exclusion chromatography

Gel filtration chromatography was carried out in a Superdex 200 HR 10/30 column (GE Healthcare), as previously described [10]. Briefly, samples (100 μl) containing 150 μg of protein in

running buffer (50 mM Tris pH 8.0, 150 mM NaCl), were individually applied to the column equilibrated with running buffer and eluted in the same buffer at a flow rate of 0.5 ml min^{-1}. Fractions of 1 ml were collected and analyzed by SDS-PAGE to confirm the identity of each peak. Protein elution profiles were monitored by measuring the absorbance at OD_{280} and analyzed with the program UNICORN 5.10.

2.7 Immunodetection of NblR

Purified NblR was used to produce anti-NblR rabbit polyclonal antibodies (Abyntek, Bizkaia, Spain) that were affinity purified with a NblR-inmobilized column. For crude protein extracts, cells from a 15 ml of *S. elongatus* cultures at OD_{750} = 0.5 were harvested by centrifugation at 7300 *g* for 5 min. Pellets were resuspended in 100 µl of lysis buffer (50 mM Tris-HCl pH 7.4, 4 mM EDTA, 0.5 mM PMSF, 0.5 mM Benzamidine, 1 mM DTT), and 50 µl of 100 µm glass beads were added. The mixture was homogenized with four cycles of 10 s in a Minibeadbeater. The cell lysate was centrifuged at 8000 *g* for 4 min at 4 °C, and the supernatant fraction transferred to a new tube. Protein concentration was estimated by the Bradford method.

For NblR immunodetection, 30 µg/lane of crude protein extracts were electrophoresed in a SDS-PAGE gradient gel (6-15% acrylamide) and transferred to PVDF membranes using a semidry transfer system. Membranes were blocked in TBS (20 mM Tris pH 7.5, 500 mM NaCl) containing 5% (w/v) BSA. Filters were then incubated in the presence of anti-NblR in TBS and subsequently with ECL Rabbit IgG, HRP-Linked F(ab')2 Fragment (from donkey) (GE Healthcare). Immunoreactive bands were detected using the ECL Plus Western Blotting Detection Kit (GE Healthcare) and scanning in a Typhoon 9410 fluorescence imaging system (GE Healthcare) using 488nm/520BP40 laser/filter. A control of the total amount of loaded protein and transfer was obtained after membrane staining with Fast Green (FCF).

2.8. Electrophoretic gel mobility shift assays

The DNA probe for *nblA* was obtained by PCR using nblA-2F and nblA-2R (positions -296 to -46 relative to the transcriptional start site) from *S. elongatus* genomic DNA. *rpoD5* control probe was obtained by PCR using rpoD5-1R and rpoD5-1F (positions -223 to +4). Double-stranded DNA fragments were 5′ end-labeled with ^{32}P using T4 polynucleotide kinase (Takara). Binding reactions were performed by mixing recombinant NblR, $NblR^{C69A}$ or $NblR^{C96A}$ (from 7.6 to 191.27 pmol) with 50 fmol of labelled probe and 1 μg of poly(dI-dC) in a final volume of 20 μl of binding buffer (20 mM HEPES, pH 8, 50 mM NaCl, 5 mM $MgCl_2$, 0.1 mM EDTA, 100 mM DTT and 5% glycerol), at 4 °C for 30 min. DNA–protein complexes were resolved on a native 6% polyacrylamide gel, run at 100 V and 4 °C for approximately 1 h and visualized on the Fuji Film FLA3000 gel imaging system.

2.9. Circular dichroism

Spectra of the wild-type and the mutants were collected on a Jasco J810 (Japan) spectropolarimeter with a Peltier unit. The instrument was periodically calibrated with (+)-10-camphorsulfonic acid. Spectra were acquired at 25 ºC in phosphate buffer at pH 7.0 (50 mM). The scan speed was 50 nm min^{-1}, with a data pitch of 0.2 nm and a band width of 1 nm. Six scans were acquired for each protein. Molar ellipticity was obtained as described [21].

2.10. Protein identification by mass spectrometry analysis

Aliquots of 25 μg of proteins were diluted up to 90 μl in 50 mM ammonium bicarbonate (pH 8.0) containing 10 mM DTT. After incubation at 60 ºC for 20 min, the samples were cooled and 10 μl of iodoacetamide was added to obtain a final iodocetamide concentration of 55 mM. The reactions proceeded for 30 min at room temperature in the dark. To determine available free thiol groups a parallel procedure was carried out in the absence of DTT. For the double thiol group

labeling experiments, aliquots of 25 µg of protein were diluted up to 80 µl in 50 mM ammonium bicarbonate (pH 8.0) containing 5.5 mM iodocetamide. After incubation at room temperature in the dark for 30 min, 10 µl of DTT were added to obtain a final concentration of 10 mM. Reduction proceeded for 20 min at 60 ºC and, after cooling the sample, 10 µl of 4-vinylpyridine were added to a final concentration of 100 mM. Afterwards, samples were digested with sequencing grade trypsin (Promega) as described [22], and subject to peptide mass Fingerprinting.

The digestion mixture was dried in a vacuum centrifuge, resuspended in 7 µl of 0.1% TFA (trifluoroacetic acid, Sigma), and 1 µl was spotted onto the MALDI target plate. After the droplets were air-dried at room temperature, 0.5 µl of matrix (5 mg ml^{-1} CHCA α-cyano-4-hydroxycinnamic acid, Sigma) in 0.1% TFA-ACN/H_2O (1:1, v/v) was added and allowed to air-dry at room temperature. The resulting samples were analyzed in a 4700 Proteomics Analyzer (AB SCIEX, Foster City, USA) in positive reflectron mode (3000 shots every position). The spectra were normalized by the maximum intensity peak. The match of the peaks corresponding to protein peptides was done with mMass [23] taking into account as variable modifications: the oxidation or dethiomethylation of Met residues, and the carbamidometylation of Cys, Lys, His, Asp, Glu or N-terminal residues.

3. Results and Discussion

3.1. In vivo effect of mutations Cys69Ala and Cys96Ala at NblR

To investigate a possible regulatory role of Cys69 and Cys96 during acclimation to stress, we constructed *S. elongatus* strains in which Cys69, Cys96 or both cysteine residues were replaced by alanine. Strains NblR^{C69A}-RCS3, NblR^{C96A}-RCS3 and NblR$^{C69A/C96A}$-RCS3 (Table 1) were generated following exactly the same strategy for allelic replacement used in a previous work [10]. A streptomycin-resistant control strain retaining the wild-type *nblR* allele (WT-RCS3) was generated in parallel. Homozygosis for C.S3 alleles was promptly achieved in all strains (data not shown).

To determine the impact of substitutions on NblR function, we analysed the ability of *nblR* point mutant derivatives of *S. elongatus* to respond to two situations known to trigger phycobilisome degradation, that is, starvation for nitrogen or for sulphur (Fig. 2 A and 2 B). The response of NblR^{C69A}-RCS3, NblR^{C96A}-RCS3 and NblR$^{C69A/C96A}$-RCS3 to each type of stress was similar. All three strains lost their pigments at a significantly slower rate than the wild-type control strain, but still retained considerable NblR activity, as inferred by comparison with the NblR^{-} strain (Fig. 2). In both types of nutrient stress, the double mutant (*nblR*$^{C69A/C96A}$) was slightly more impaired than each of the two single mutants, suggesting that the effect of point mutations was additive.

To confirm that the differences in pigment content between wild-type and point mutation strains were due to differences in the levels of *nblA* gene activation by the different NblR derivatives, *nblA* promoter activity was compared. To this end, strains carrying the P$_{nblA}$::*luxAB* fusion were obtained and subjected to nitrogen or sulfur deprivation and their bioluminescence determined at different time intervals. As shown in Fig. 3, all three mutant proteins had a significant impact on reporter expression, and again the double mutant *nblR*$^{C69A/C96A}$ was more impaired in reporter induction than any of the single mutants under each type of stress.

The reduced activity inferred for the NblR mutant proteins made us wonder whether their intracellular levels were reduced *in vivo*, particularly under stress conditions. To investigate this issue, we performed western blots with extracts from wild-type and *nblR* mutant derivative strains subjected to nitrogen deprivation. No significant differences in NblR protein levels were obtained between the control strain and *nblR*^{C69A} or *nblR*^{C96A} derivatives, indicating that the individual mutations did not have a significant impact on the protein levels. On the other hand, small but detectably lower levels of NblR protein could be observed from *nblR*$^{C69A/C96A}$ cultures (Fig. 4 and data not shown), suggesting that the corresponding protein was less stable *in vivo*.

3.2. *In vitro* characterization of NblR and mutant derivatives

Wild-type and mutant derivatives of NblR carrying C69A or C96A substitutions were obtained with a six histidine N-terminal tag, overexpressed in *E. coli* and purified as described [10].

3.2.1. Structural characterization of the proteins by circular dichroism spectroscopy

Changes in the secondary structure of the NblR, NblR^{C69A} and NblR^{C96A} proteins by far-UV CD were investigated. As shown in Figure 5, the shape of the spectrum was basically the same for all three proteins, consistent with no main changes in secondary structure. The small increases in the ellipticity values at 222 nm for the mutant proteins (when compared to the spectrum of the wild-type protein) could be due to the removal of the cysteine residues, or alternatively to small conformational changes of the neighbouring aromatic side chains, which also absorb at 222 nm [24]. The NblR modelled structure (Fig. 1) suggests that the packing of the side chains of several phenylalanine and tyrosine residues could be altered in the mutant proteins. Particularly important are Phe68, which is preceding Cys69, and Tyr104, a key residue in the dimerization interface whose mutation to alanine confers a null phenotype (Supplementary Figure). Thus, the small differences in

the far-UV spectra between NblR and mutant derivatives are most probably due to changes in the packing of nearby aromatic residues, and/or removal of the cysteine residues.

3.2.2. Free thiol groups in NblR, NblR^{C69A} and NblR^{C96A} proteins

The possible involvement of Cys69 and Cys96 in disulphide bridges was analyzed by mass spectrometry with NblR, NblR^{C69A} and NblR^{C96A}. Since iodoacetamide reacts only with free thiol groups, the previous addition of DTT to protein ensures that all thiol groups are reduced and therefore accessible before addition of iodoacetamide. Thus, a normalized ratio of the intensity of the peaks from the Cys-containing peptides with and without DTT treatment would reflect the degree of accessibility of free thiols. As shown in Fig. 6, DTT increased the intensity of six out of eight peaks in NblR, NblR^{C69A} and NblR^{C96A} samples, indicating that although the Cys residues were not accessible in the corresponding proteins, they were not forming disulphide bridges in NblR. Consistent with this, disulphide cross-linked peptides were not detected during the mass spectrometry analysis of NblR.

Next, we performed double labeling experiments in which the free thiol groups of NblR were first blocked with iodoacetamide and then treated with DTT previously to the (potential) blocking with 4-vinylypyridine of DTT-freed thiol groups. Failure to detect peptides modified with the latter reagent (not shown) confirmed the absence of disulphide bonds in the NblR samples. Therefore, Cys69 and Cys96 of NblR do not seem to form intra or intermolecular disulphide bonds, at least under the experimental conditions tested.

3.2.3. Size-exclusion chromatography analysis of NblR, NblRC69A and NblRC96A proteins

To investigate a possible impact of C69A and C96A substitutions on the oligomeric state and the shape (and then, a potential partial unfolding) of NblR, size-exclusion chromatography analysis was performed with NblR, NblR^{C69A} and NblR^{C96A}. From our structural studies in CD

(section 3.2.1.), it could be anticipated that similar elution volumes should be obtained for the three proteins. All three proteins eluted as homogeneous peaks with identical profiles and elution volumes centered at 16.6 ml (Fig. 7). The calculated molecular mass of 28.000 Da clearly matched the predicted molecular weight of NblR (28.590 Da). As previously shown for NblR [10], reducing (DTT) or oxidant conditions (Cu-phenantroline) did not affect the elution profile of $NblR^{C69A}$ or $NblR^{C96A}$ (data not shown). Thus, the results are consistent with the monomeric state of NblR and the lack of involvement of the Cys residues in intra or intermolecular disulphide bridges.

3.2.4 Binding of NblRC69A and NblRC96A proteins to the nblA promoter

To test the effect of the C69A and C96A substitutions on NblR binding to DNA, we carried out mobility-shift assays using control and mutant derivatives of NblR and a fragment corresponding to the complex regulatory region of *nblA* (-296 to -46 relative to the translation start). It should be noted that specific sites or consensus sequences for NblR binding are not known and detection of band-shifts have only been observed with very concentrated NblR protein and relatively large DNA fragment [9].

As shown in Fig. 8, we were able to distinguish up to five band shifts with 9.56 μmolar of NblR, a result suggesting that this region contain several binding sites for NblR. When $NblR^{C69A}$ and $NblR^{C96A}$ proteins were used, less band-shifts were observed. In addition, bands shifted by $NblR^{C96A}$ and, to a greater extent by $NblR^{C69A}$, run faster and more diffuse than the fully retarded bands obtained with NblR. Thus, it appears that purified $NblR^{C69A}$ and $NblR^{C96A}$ proteins show decreased affinity for the *nblA* promoter region (Fig. 8, and data not shown). The specificity of the binding was supported by the lack of band-shifts in a parallel assay with a probe of similar size corresponding to the *rpoD5* promoter region (Fig. 8, control lines). Taken together, our results strongly suggest that the inability of the $NblR^{C69A}$-RCS3 and $NblR^{C96A}$-RCS3 strains to achieve

maximal activation of the *nblA* gene under stress conditions is due to slightly impaired interactions with the *nblA* regulatory region.

Most regulatory DNA-binding proteins are dimers (or higher oligomers) because dimerization allows cooperativity and therefore decreases the effective protein concentration for binding to target sequences. However, we have only found evidence of the monomeric state of NblR. Since the high concentration of NblR proteins required for gel-shift experiments suggests that the *in vitro* complexes of NblR with the *nblA* regulatory region contain a lower affinity (inactive) conformation of NblR, additional factors, absent in the *in vitro* assays may contribute to NblR binding. The mechanism leading to NblR activation, and whether it involves homodimerization as in other RRs from the OmpR/PhoB family [15] and/or interaction with other proteins, remains to be understood.

4. Conclusions

Although residues Cys69 and Cys96 of NblR are predicted to be located at an appropriated distance to form a disulphide bridge between α-helices 3 and 4, and could thus play a regulatory role by redox sensing, our analyses clearly exclude this as the main mechanism for NblR activation. Mutations C69A and C96A had basically no impact on NblR structure, as observed by far-UV CD, size and oligomerization state (as shown by size exclusion chromatography), or modest impact on NblR function, as determined by analysis of pigment content, reporter expression and DNA binding. No evidence of disulphide bridge formation within NblR could be obtained and, although we cannot safely exclude that disulphide bridges could form *in vivo*, it is clear that bridge formation is not required for maximal NblR activation. However, the possibility of redox regulation of the NblR activity is not definitively excluded here, since the moderate effect produced by the mutations on NblR function open the door to other modifications of the NblR cysteines and/or intermolecular disulfide bonds with hypothetical protein(s) could take place *in vivo*.

5. Acknowledgements

We thank M. Sánchez del Pino for mass spectrometry analysis. This work was supported by the Spanish Ministerio de Ciencia e Innovación (grants BFU2009-07371 to A.C., BIO2009-10872 and BIO2010-15424 to A.M and SAF2008-05742-C02-01 and CSD2008-00005 to J.L.N.) and the Generalitat Valenciana (grants ACOMP2006/083 and ACOMP2011/211 to A.C, ACOMP2010/114 and ACOMP2011/113 to J.L.N.). M.L. López-Redondo was a fellow of the Fundación Mutua Madrileña Automovilística. Proteomic analysis was performed in the proteomics service of the "Principe Felipe" Research Centre (CIPF), Valencia (Spain), a member of ProteoRed. The authors declare they do not have any competing interest.

6. References

[1] A.R. Grossman, M.R. Schaefer, G.G. Chiang, J.L. Collier, The phycobilisome, a light-harvesting complex responsive to environmental conditions, Microbiol Rev 57 (1993) 725-749.

[2] J.L. Collier, A.R. Grossman, Chlorosis induced by nutrient deprivation in Synechococcus sp. strain PCC 7942: not all bleaching is the same, J Bacteriol 174 (1992) 4718-4726.

[3] J.L. Collier, A.R. Grossman, A small polypeptide triggers complete degradation of light-harvesting phycobiliproteins in nutrient-deprived cyanobacteria, Embo J 13 (1994) 1039-1047.

[4] A.R. Grossman, D. Bhaya, Q. He, Tracking the light environment by cyanobacteria and the dynamic nature of light harvesting, J Biol Chem 276 (2001) 11449-11452.

[5] R. Schwarz, A.R. Grossman, A response regulator of cyanobacteria integrates diverse environmental signals and is critical for survival under extreme conditions, Proc Natl Acad Sci U S A 95 (1998) 11008-11013.

[6] M.K. Ashby, J. Houmard, Cyanobacterial two-component proteins: structure, diversity, distribution, and evolution, Microbiol Mol Biol Rev 70 (2006) 472-509.

[7] E. Sendersky, R. Lahmi, J. Shaltiel, A. Perelman, R. Schwarz, NblC, a novel component required for pigment degradation during starvation in Synechococcus PCC 7942, Mol Microbiol 58 (2005) 659-668.

[8] P. Salinas, D. Ruiz, R. Cantos, M.L. Lopez-Redondo, A. Marina, A. Contreras, The regulatory factor SipA provides a link between NblS and NblR signal transduction pathways in the cyanobacterium *Synechococcus* sp. PCC 7942, Mol Microbiol 66 (2007) 1607-1619.

[9] I. Luque, G. Zabulon, A. Contreras, J. Houmard, Convergence of two global transcriptional regulators on nitrogen induction of the stress-acclimation gene *nblA* in the cyanobacterium *Synechococcus* sp. PCC 7942, Mol Microbiol 41 (2001) 937-947.

[10] D. Ruiz, P. Salinas, M.L. Lopez-Redondo, M.L. Cayuela, A. Marina, A. Contreras, Phosphorylation-independent activation of the atypical response regulator NblR, Microbiology 154 (2008) 3002-3015.

[11] Y. Ohashi, W. Shi, N. Takatani, M. Aichi, S. Maeda, S. Watanabe, H. Yoshikawa, T. Omata, Regulation of nitrate assimilation in cyanobacteria, J Exp Bot 62 (2011) 1411-1424.

[12] H. Kato, T. Chibazakura, H. Yoshikawa, NblR is a novel one-component response regulator in the cyanobacterium *Synechococcus elongatus* PCC 7942, Biosci Biotechnol Biochem 72 (2008) 1072-1079.

[13] C.M. Dyer, F.W. Dahlquist, Switched or not?: the structure of unphosphorylated CheY bound to the N terminus of FliM, J Bacteriol 188 (2006) 7354-7363.

[14] A. Toro-Roman, T.R. Mack, A.M. Stock, Structural analysis and solution studies of the activated regulatory domain of the response regulator ArcA: a symmetric dimer mediated by the alpha4-beta5-alpha5 face, J Mol Biol 349 (2005) 11-26.

[15] R. Gao, T.R. Mack, A.M. Stock, Bacterial response regulators: versatile regulatory strategies from common domains, Trends Biochem Sci 32 (2007) 225-234.

[16] E. Hong, H.M. Lee, H. Ko, D.U. Kim, B.Y. Jeon, J. Jung, J. Shin, S.A. Lee, Y. Kim, Y.H. Jeon, C. Cheong, H.S. Cho, W. Lee, Structure of an atypical orphan response regulator protein supports a new phosphorylation-independent regulatory mechanism, J Biol Chem 282 (2007) 20667-20675.

[17] J.M. Hickey, L. Weldon, P.S. Hefty, The atypical OmpR/PhoB response regulator ChxR from Chlamydia trachomatis forms homodimers in vivo and binds a direct repeat of nucleotide sequences, J Bacteriol 193 (2011) 389-398.

[18] J. Sauer, M. Gorl, K. Forchhammer, Nitrogen starvation in *synechococcus* PCC 7942: involvement of glutamine synthetase and NtcA in phycobiliprotein degradation and survival, Arch Microbiol 172 (1999) 247-255.

[19] S.S. Golden, L.A. Sherman, Optimal conditions for genetic transformation of the cyanobacterium Anacystis nidulans R2, J Bacteriol 158 (1984) 36-42.

[20] J. Espinosa, K. Forchhammer, A. Contreras, Role of the *Synechococcus* PCC 7942 nitrogen regulator protein PipX in NtcA-controlled processes, Microbiology 153 (2007) 711-718.

[21] M.L. Lopez-Redondo, A. Contreras, A. Marina, J.L. Neira, The regulatory factor SipA is a highly stable beta-II class protein with a SH3 fold, FEBS Lett 584 (2010) 989-994.

[22] A. Shevchenko, O.N. Jensen, A.V. Podtelejnikov, F. Sagliocco, M. Wilm, O. Vorm, P. Mortensen, H. Boucherie, M. Mann, Linking genome and proteome by mass spectrometry: large-scale identification of yeast proteins from two dimensional gels, Proc Natl Acad Sci U S A 93 (1996) 14440-14445.

[23] M. Strohalm, M. Hassman, B. Kosata, M. Kodicek, mMass data miner: an open source alternative for mass spectrometric data analysis, Rapid Commun Mass Spectrom 22 (2008) 905-908.

[24] R.W. Woody, Circular dichroism, Methods Enzymol 246 (1995) 34-71.

[25] D. Hanahan, Techniques for transformation of *Escherichia coli.*, in: e. Glover D (Ed.), DNA cloning, IRL Press, Oxford, UK, 1985, pp. 109–135.

TABLE 1. Strains and plasmids used in this work.

Strain or plasmid	Genotype or relevant characteristics	Source or reference
E. coli DH5α	F^- ϕ80d*lacZ*ΔM15Δ(*lacZYA-argF*)U169 *endA1 recA1 hsdR17*(r_K^- m_K^+) *deoR thi-1 supE44 gyrA96 relA1* λ^-	[25]
E. coli BL21-CodonPlus (DE3)-RIL	F^- *ompT hsdS*(r_B^- m_B^-) dcm^+ Tet^r *gal* λ(DE3) *endA* Hte [*argU ileY leuW* Cam^r]	Stratagene
Synechococcus sp. PCC 7942	Wild-type *S. elongatus* PCC 7942	Pasteur culture collection
Synechococcus NblR45	$NblR^-$, Km^r	[9]
Synechococcus WT-RCS3	C.S3 downstream *nblR*, Sm^r	This work
Synechococcus $NblR^{C69A/C96A}$-RCS3	$NblR^{C69A-C96A}$, Sm^r	This work
Synechococcus $NblR^{C96A}$-RCS3	$NblR^{C69A}$, Sm^r	This work
Synechococcus $NblR^{C69A}$-RCS3	$NblR^{C96A}$, Sm^r	This work
Synechococcus WT-RCS3-C103	P*nblA*::*luxAB* into NSII, Sm^r Cm^r	This work
Synechococcus NblR-45-C103	$NblR^-$, P_{nblA} : : *luxAB*, Km^r Cm^r	[8]
Synechococcus $NblR^{C69A/C96A}$-RCS3-C103	$NblR^{C69A/C96A}$, P_{nblA} : : *luxAB*, Km^r Cm^r	This work

Synechococcus NblR^{C96A}-RCS3-C103	NblR^{C96A}, P$_{nblA}$: : *luxAB*, Km^r Cm^r	This work
Synechococcus NblR^{C69A}-RCS3-C103	NblR^{C69A}, P$_{nblA}$: : *luxAB*, Km^r Cm^r	This work
pENS45	*nblR*::CK2, Ap^r Kmr	[9]
pENS38	pPROEX-HTb encoding 6His-NblR, Ap^r	[9]
pENS38_1	pENS38 with *nblR*^{C69A}	This work
pENS38_2	pENS38 with *nblR*^{C96A}	This work
pUAGC235	pBluescriptII SK(+) with *nblR*, Ap^r	[10]
pUAGC453	pBluescriptII SK(+) with CS3, Ap^r Sm^r	[10]
pUAGC236	pUAGC235 with C.S3 downstream *nblR*, Ap^r Sm^r	This work
pUAGC237	pUAGC236 with *nblR* downstream sequences, Ap^r Sm^r	This work
pUAGC733	pUAGC237 with *nblR*^{C69A}	This work
pUAGC734	pUAGC237 SK(+) with *nblR*^{C96A}	This work
pUAGC735	pUAGC237 with *nblR*$^{C69A-C96A}$	This work
pUAGC103	pAM1580 with P*nblA*::*luxAB*, Ap^r Cm^r	[20]

7. Figure Legends

FIGURE 1. Structure of the NblR receiver domain. Ribbon representation of the three-dimensional model of NblR receiver domain [10]. Relevant residues are shown as ball-and-stick and the possible disulphide bridge is denoted by a black broken line. The structural elements involved in the dimerization surface in the OmpR/PhoB family are highlighted in a dark hue, and labeled.

FIGURE 2. Pigment degradation in NblR mutants. (1) Time curse of PBS degradation plotted as a function of time in strains starved for nitrogen (left) or sulfur (right) during 72 hours. WT (□), $NblR^{-}$ (○), $NblR^{C69A}$ (▽), $NblR^{C96A}$ (◇) and $NblR^{C69A/C96A}$ (△). A representative experiment out of three is shown. (2) Visual appearance of the same cultures after 1 ml cell aliquots were removed and photographed at the indicated times of starvation.

FIGURE 3. Induction of nblA::luxAB in NblR mutant strains. Bioluminiscence activity (Relative Light Units) is plotted as a function of time in strains starved for nitrogen (-N) or sulfur (-S). In each case, a representative assay out of three, is shown. Figure legends as in Fig. 1.

FIGURE 4. Effect of nblR mutations on protein expression levels. Immunodetection of NblR in protein extracts obtained 12 hours after transfer of cultures from nitrate to nitrogen-free media. The inmunodetected NblR is indicated by a black arrowhead. For each lane the protein loading control, after membrane staining, is shown.

*FIGURE 5. Structural characterization of the proteins***.** Far-UV CD spectra of NblR, $NblR^{C69A}$ and $NblR^{C96A}$ proteins.

FIGURE 6. Mass spectrometry analysis of NblR, NblR^{C69A} and NblR^{C96A}. Peptide mass fingerprinting were obtained from samples treated with or without DTT. The accessibility ratio (DTT/no DTT) was calculated for each peptide by dividing the normalized peak intensities in the DTT-treated sample by that in the not treated sample. The ratios are plotted as a function of the mass of the peptides. Peptides containing residues 69 and 96 are colored in blue and red, respectively. Wild-type peptides (containing Cys residues) are indicated with filled circles whereas mutant peptides (containing Ala residues) are indicated with empty circles.

FIGURE 7. Gel filtration analysis of NblR, NblR^{C69A} and NblR^{C96A} proteins. Recombinant purified NblR(—), NblR^{C69A} (···) and NblR^{C96A} (–·–) at 54 µM were subjected to analytical size exclusion chromatography. In the inset, the NblR elution volume is indicated (♦) in a molecular standard curve generated using β-amylase, Alcohol Dehydrogenase (ADH), Serum Albumin (Albumin), Carbonic Anhydrase (CA) and Cytochrome c (Cit C).

FIGURE 8. Gel retardation of the nblA promoter region by NblR, NblR^{C69A} and NblR^{C96A}. A ^{32}P-end-labelled DNA sequence of the -296 to -46 region of *nblA* (0.05 pmol) was used as probe and incubated with increasing concentrations (0.38, 3.8 and 9.56 µM) of NblR, NblR^{C69A} and NblR^{C96A} in the presence of an excess of unspecific poly(dI-dC) DNA. For the control assay NblR and a DNA fragment of the -223 to +4 region of *rpoD5* were used instead. Complexes were electrophoreticaly separated using 6% native polyacrylamide gels. While and black arrowheads indicate, respectively, the *nblA* DNA probe and retarded bands.

Fig.1

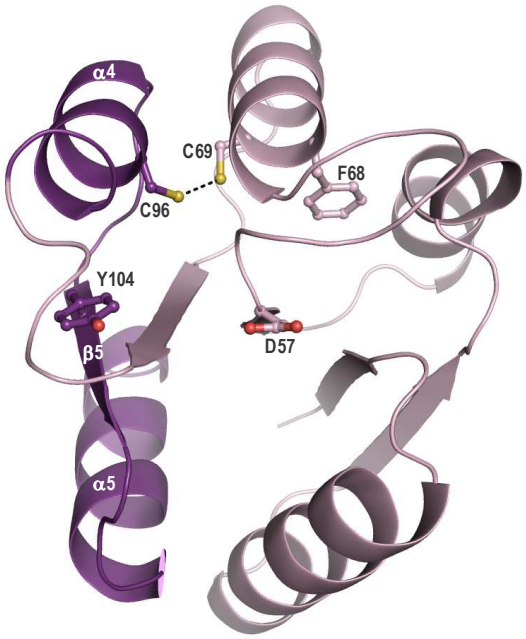
α4
C69
F68
C96
Y104
D57
β5
α5

Fig.2

A

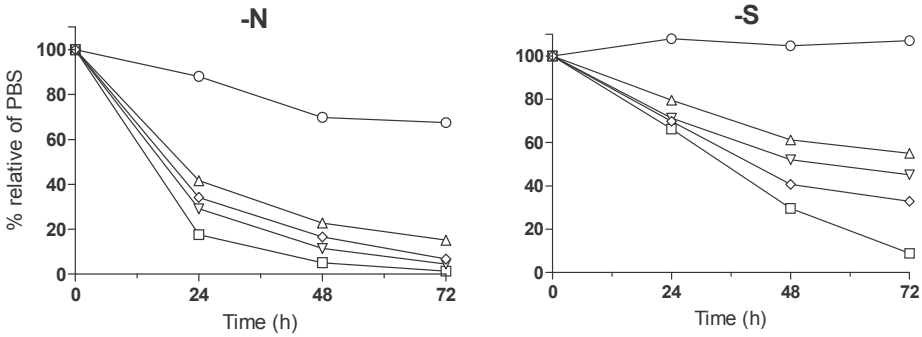
-N
-S
% relative of PBS
100
80
60
40
20
0
0
24
48
72
Time (h)

B

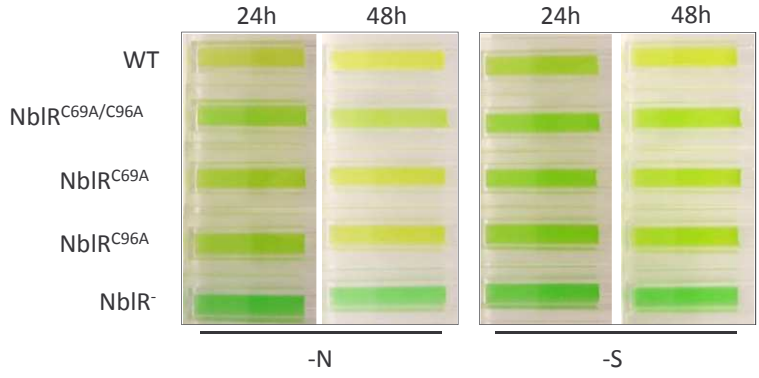
24h
48h
24h
48h
WT
NblR^C69A/C96A
NblR^C69A
NblR^C96A
NblR^-
-N
-S

Fig.3

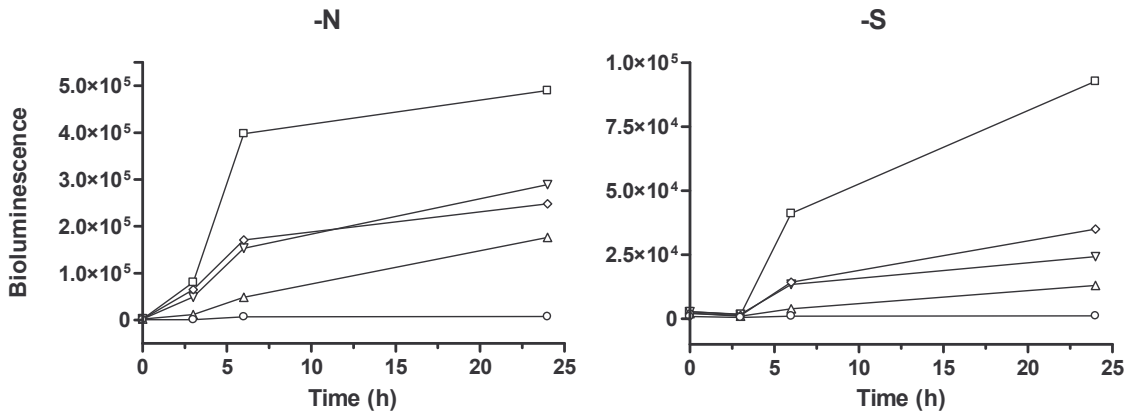
-N
-S
Bioluminescence
5.0×10⁵
4.0×10⁵
3.0×10⁵
2.0×10⁵
1.0×10⁵
0
1.0×10⁵
7.5×10⁴
5.0×10⁴
2.5×10⁴
0
0
5
10
15
20
25
Time (h)
Time (h)

Fig.4

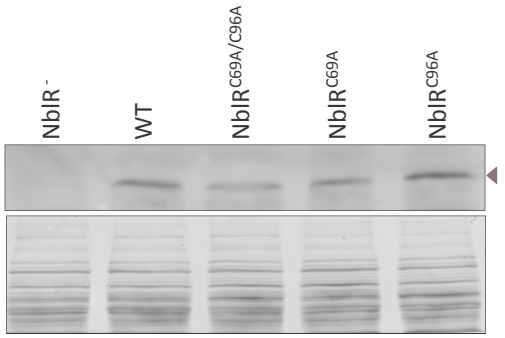
NblR⁻
WT
NblR^C69A/C96A
NblR^C69A
NblR^C96A

Fig.5

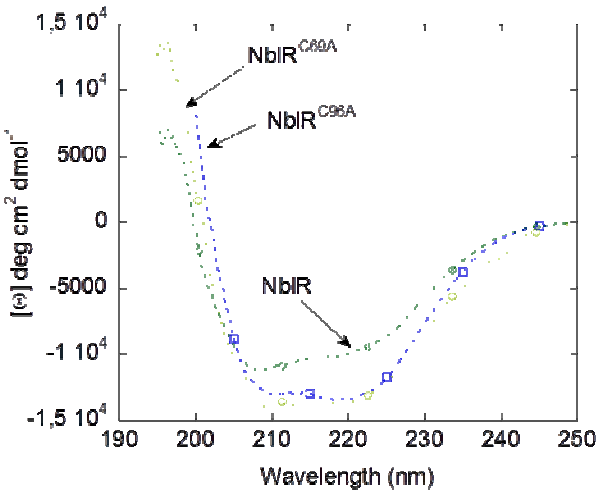
1,5 10^4
1 10^4
5000
0
-5000
-1 10^4
-1,5 10^4
[Θ] deg cm^2 dmol^-1
NblR^C69A
NblR^C96A
NblR
190
200
210
220
230
240
250
Wavelength (nm)

Fig.6

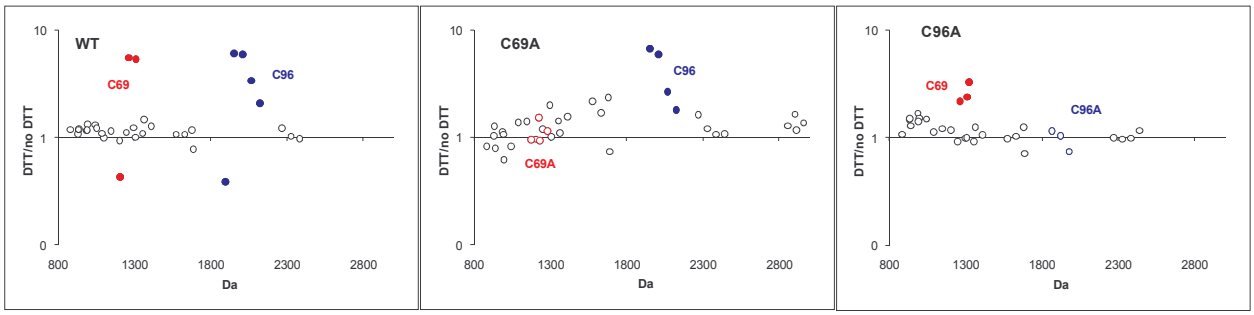
WT
C69
C96
C69A
C96
C69A
C96A
C69
C96A
DTT/no DTT
10
1
0
800
1300
1800
2300
2800
Da

Fig.7

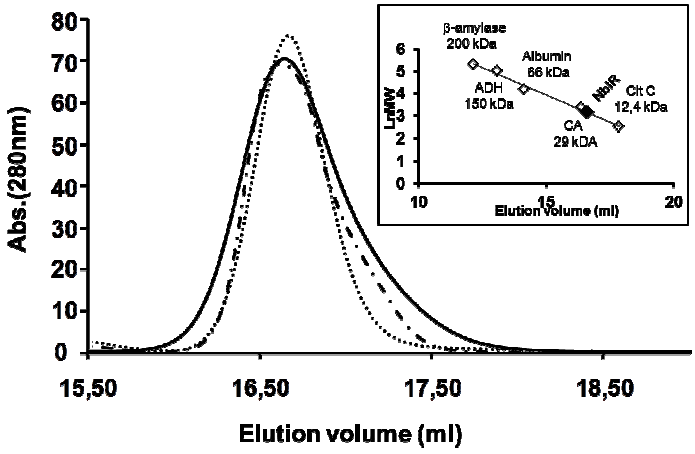
Abs.(280nm)
80
70
60
50
40
30
20
10
0
15,50
16,50
17,50
18,50
Elution volume (ml)
β-amylase
200 kDa
Albumin
66 kDa
ADH
150 kDa
NblR
Cit C
12,4 kDa
CA
29 kDA
LnMW
6
5
4
3
2
1
0
10
15
20
Elution volume (ml)

Fig.8

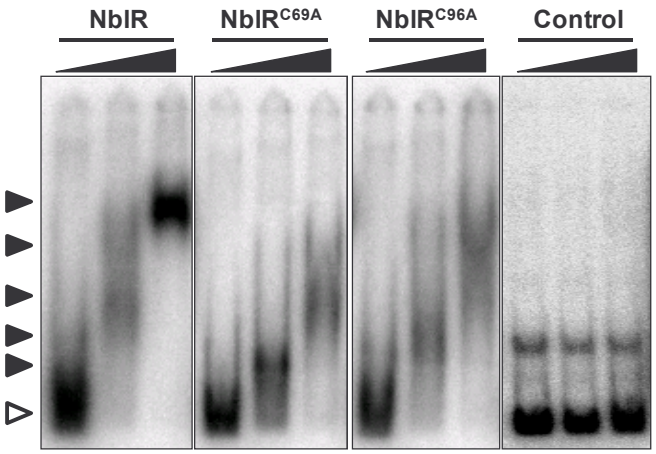
NblR
NblR^C69A
NblR^C96A
Control

Supplementary Figure

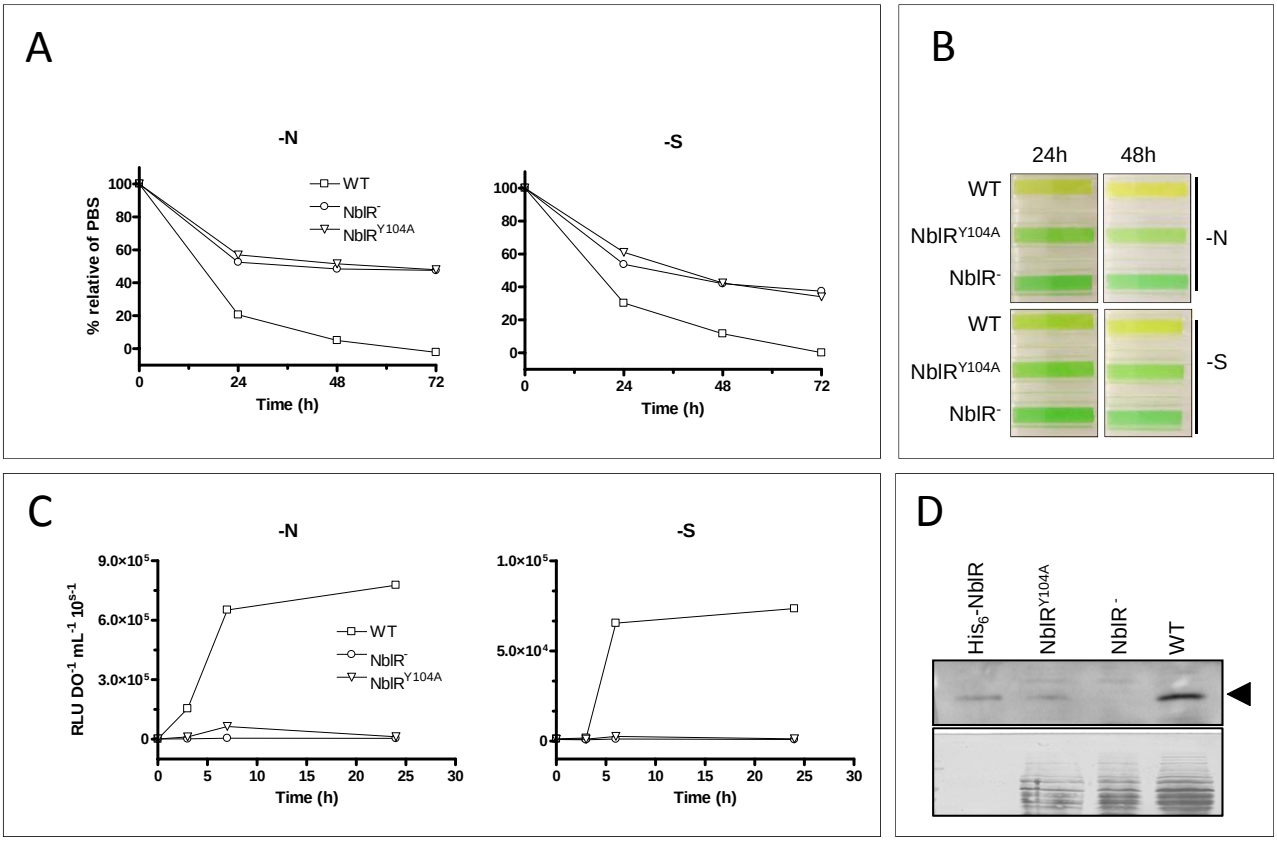

I*n vivo* analysis of the effect of Y104A point mutation on NblR function/properties. A) Time course PBS degradation B) Visual appearance of cultures C) Induction profile of *nblA::luxAB* and D) immunodetection of NblR. Additional details see main text.

Supplementary Table. Oligonucleotides.

Name	Sequence (5’-3’)
NblR-down-4F	5’-TGTAGAAGCTTGCGGCTC-3’
NblR-down-4R	5’-CTTTAGGTCGACTGCAGTCTCGTCATC-3’
NblR-C69A-F	5´-AATCAGGTCTGCAATTCGCCCGACAGCTGCGCGATC-3’
NblR-C69A-R	5´-GATCGCGCAGCTGTCGGGCGAATTGCAGACCTGATT-3’
NblR-C96A-F	5´-CGTTGAAGACCGCGTTGCCGCTCTCGAAGCAGGGGCTGAT-3’
NblR-C96A-R	5´-ATCAGCCCCTGCTTCGAGAGCGGCAACGCGGTCTTCAACG-3’
NblR-1F	5´-GAGTGAGGAAGAATTCTGATCGCGCCAGCCTC-3’
NblR-1R	5’ -CTCTCGCGTCGACACTTAGCGCGGATGCTC-3’
CS3-2F	5´-ACAAAACGGTTTACCAGCAT-3’
pAM1580seq	5´-CCATTTCTGGCGTACGGC-3’
nblA-1F	5´-CTCTGAAACAGTTGCTGTCTGA-3’
rpoD5-1F	5'- CAAGAAACCAAGCACTGAAC-3'
rpoD5-1R	5'- CCGTCATGGTGAATATCCAG-3'
nblA-2F	5'-CTGTTTCAGAGTCTTTCTGAATTG-3'
nblA-2R	5'- GGGGGATCTGTGGCTGTTCC-3'